This method can also be particularly powerful in cases where the EPR spectrum is very poorly resolved and yields no information, as is the case with the neutral paramagnetic compound $[(\eta^5\text{-}C_5Me_5)Zr(cot)]$;[22] ENDOR then becomes valuable in supplying the desired information without necessarily resorting to X-ray diffraction methods. Proton and ^{91}Zr ENDOR studies on the latter compound are under way.

Registry No. [CpTi(cht)], 51203-49-7; $[CpTi(cht)]^-$, 115338-78-8; $[(\eta^5\text{-}C_5D_5)Ti(cht)]$, 115338-79-9; $[(\eta^5\text{-}C_5D_5)Ti(cht)]^-$, 115338-80-2; THF, 109-99-9.

---

(22) Blenkers, J.; Bruin, P.; Teuben, J. H. *J. Organomet. Chem.* **1985**, *297*, 61.

Contribution from the Department of Chemistry,
Queen's University, Kingston, Canada K7L 3N6

Carbon Monoxide and Carbon Dioxide Hydrogenation Catalyzed by Supported Ruthenium Carbonyl Clusters. A Novel Procedure for Encapsulating $Ru_3(CO)_{12}$ within the Pores of Na–Y Zeolite

W. Ross Hastings, Charles J. Cameron, Marian J. Thomas, and Michael C. Baird*

Received December 23, 1987

Zeolite-supported ruthenium catalysts for the hydrogenation of carbon monoxide and carbon dioxide have been prepared by sorbing $Ru(CO)_5$ (molecular diameter 6.3 Å) onto Na–Y zeolite and Linde 5A molecular sieve. Although the metal carbonyl is not absorbed into the pores of the molecular sieve (diameter 4.2 Å), it is readily absorbed into the pores (diameter 7.4 Å) and supercages (diameter 13 Å) of the Na–Y zeolite. The $Ru(CO)_5$ in Na–Y converts in the absence of carbon monoxide to the much larger $Ru_3(CO)_{12}$ (diameter 9.2 Å), which remains on the surface of the molecular sieve but is trapped within the supercages of the Na–Y zeolite because it cannot pass through the smaller pores. Slow, temperature-programmed heating of the $Ru_3(CO)_{12}$ in Na–Y to 350 °C under a flow of hydrogen results in decarbonylation and formation of a CO hydrogenation catalyst that produces a very atypical (for ruthenium) hydrocarbon distribution truncated at about C_{10}. The unusual product distribution presumably arises because the catalyst sites are situated within the zeolite supercages. Thus the metal is highly dispersed and/or the growing hydrocarbon chains are subject to geometrical limitations on their growth. Consistent with this hypothesis, ruthenium carbonyl clusters immobilized on the external surfaces of Na–Y zeolite, Linde 5A molecular sieve, and γ-alumina all exhibit typical, nonselective hydrocarbon product distributions. The same supported ruthenium carbonyl clusters are also extremely active catalysts for the selective hydrogenation of CO_2 (H_2:CO_2 = 4:1) to methane. At a lower H_2:CO_2 ratio (1:1), however, Na–Y-supported $Ru_3(CO)_{12}$ catalyzes the hydrogenation of CO_2 to higher hydrocarbons as well (up to C_{16}). Interestingly, CO_2 hydrogenation differs from CO hydrogenation in that the former process (a) yields no olefins or isoalkanes, both of which are prominent from CO hydrogenation, and (b) does not result in a product distribution exhibiting the depletion in C_2 products normally obtained from CO hydrogenation. In spite of these apparently significant differences, it is argued that CO_2 hydrogenation involves initial reduction of the CO_2 to CO and that hydrogenation of both proceeds via the same carbidic mechanism proposed elsewhere.

In recent years, considerable research has been directed toward gaining a better understanding of reactions involving the ruthenium–catalyzed hydrogenation of carbon monoxide[1] and dioxide.[2] Catalysts formed by supporting both inorganic ruthenium salts[3] and ruthenium carbonyl clusters[2c,k,3g,h,4] on simple oxides have been shown to reduce CO to a wide variety of products, and there have also been a number of publications dealing with CO-hydrogenation catalysts containing ruthenium in zeolites and similar materials.[5] In contrast, the hydrogenation of CO_2 catalyzed by ruthenium

---

(1) For reviews, see: (a) Anderson, R. B. *The Fischer-Tropsch Synthesis*; Academic: New York, 1984. (b) King, F.; Shutt, E.; Thomson, A. I. *Platinum Met. Rev.* **1985**, *29*, 146.

(2) (a) Mill, G. A.; Steffgen, F. W. *Catal. Rev.* **1973**, *8*, 159. (b) Vlasenko, V. M.; Yuzefovich, G. E. *Russ. Chem. Rev.* (*Engl. Transl.*) **1969**, *38*, 728. (c) Karn, F. S.; Shultz, J. F.; Anderson, R. B. *Ind. Eng. Chem. Prod. Res. Dev.* **1965**, *4*, 265. (d) Lunde, P. J.; Kester, F. L. *J. Catal.* **1973**, *30*, 423. (e) Gupta, N. M.; Kamble, V. S.; Rao, K. A.; Iyer, R. M. *J. Catal.* **1979**, *60*, 57. (f) Solymosi, F.; Erdöhelyi *J. Mol. Catal.* **1980**, *8*, 471. (g) Zağli, E.; Falconer, J. L. *J. Catal.* **1981**, *69*, 1. (h) Solymosi, F.; Erdöhelyi, A.; Kocsis, M. *J. Chem. Soc., Faraday Trans. 1* **1981**, *77*, 1003. (i) Solymosi, F.; Erdöhelyi, A.; Bânsâgi, T. *J. Chem. Soc., Faraday Trans. 1* **1981**, *77*, 2645. (j) Ferkul, H. E.; Stanton, D. J.; McCowan, J. D.; Baird, M. C. *J. Chem. Soc., Chem. Commun.* **1982**, 955. (k) Ferkul, H. E.; Berlie, J. M.; Stanton, D. J.; McCowan, J. D.; Baird, M. C. *Can. J. Chem.* **1983**, *61*, 1306. (l) Weatherbee, G. D.; Bartholomew, C. H. *J. Catal.* **1984**, *87*, 352. (m) Darensbourg, D. J.; Ovalles, C. *Inorg. Chem.* **1986**, *25*, 1603.

(3) (a) Vannice, M. A. *J. Catal.* **1975**, *37*, 449. (b) King, D. L. *J. Catal.* **1978**, *51*, 386. (c) Everson, R. C.; Woodburn, E. T.; Kirk, A. R. M. *J. Catal.* **1978**, *53*, 186. (d) Ekerdt, J. G.; Bell, A. T. *J. Catal.* **1979**, *58*, 170. (e) Vannice, M. A.; Garten, R. L. *J. Catal.* **1980**, *63*, 255. (f) Kobori, Y.; Yamasaki, H.; Naito, S.; Onishi, T.; Tamaru, K. *J. Chem. Soc., Faraday Trans. 1* **1982**, *78*, 1473. (g) Kellner, C. S.; Bell, A. T. *J. Catal.* **1982**, *75*, 251. (h) Okuhara, T.; Kimura, T.; Kobayashi, K.; Mosono, M.; Yoneda, Y. *Bull. Chem. Soc. Jpn.* **1984**, *57*, 938. (i) Smith, K. J.; Everson, R. C. *J. Catal.* **1986**, *99*, 349.

(4) (a) Kobori, K.; Naito, S.; Onishi, T.; Tamaru, K. *J. Chem. Soc., Chem. Commun.* **1981**, 92. (b) Okuhara, T.; Kobayashi, K.; Kimura, T.; Misono, M.; Yoneda, Y. *J. Chem. Soc., Chem. Commun.* **1981**, 1114. (c) Kellner, C. S.; Bell, A. T. *J. Catal.* **1981**, *70*, 418. (d) Pierantozzi, R.; Valagene, E. G.; Nordquist, A. F.; Dyer, P. N. *J. Mol. Catal.* **1983**, *21*, 189. (e) Okuhara, T.; Enomoto, T.; Tamaru, H.; Misono, M. *Chem. Lett.* **1984**, 1491. (f) Doi, Y.; Miyake, H.; Yokota, A.; Soga, K. *J. Catal.* **1985**, *95*, 293. (g) Okuhara, T.; Tamaru, H.; Misono, M. *J. Catal.* **1985**, *95*, 41. (h) Jackson, S. D.; Moyes, R. B.; Wells, P. B.; Whyman, R. *J. Chem. Soc., Faraday Trans. 1* **1987**, *83*, 905.

(5) (a) Nijs, H. H.; Jacobs, P. A.; Uytterhoeven, J. B. *J. Chem. Soc., Chem. Commun.* **1979**, 180. (b) Nijs, H. H.; Jacobs, P. A.; Uytterhoeven, J. B. *J. Chem. Soc., Chem. Commun.* **1979**, 1095. (c) Elliott, D. J.; Lunsford, J. H. *J. Catal.* **1979**, *57*, 11. (d) Nijs, H. H.; Jacobs, P. A. *J. Catal.* **1980**, *66*, 401. (e) Ballivet-Tkatchenko, D.; Tkatchenko, I. *J. Mol. Catal.* **1981**, *13*, 1. (f) Blackmond, D. G.; Goodwin, J. G. *J. Chem. Soc., Chem. Commun.* **1981**, 125. (g) Gustafson, B. L.; Lunsford, J. H. *J. Catal.* **1982**, *74*, 393. (h) Leith, I. R. *J. Chem. Soc., Chem. Commun.* **1983**, 93. (i) Okuda, O.; Tatsumi, T.; Fujimoto, K.; Tominaga, H. *Chem. Lett.* **1983**, 1153. (j) Chen, Y. W.; Wang, H. T.; Goodwin, J. G.; Shiflett, W. K. *Appl. Catal.* **1983**, *8*, 303. (k) Chen, Y. W.; Wang, H. T.; Goodwin, J. G. *J. Catal.* **1983**, *83*, 415. (l) Audier, M.; Klinowski, J.; Benfield, R. E. *J. Chem. Soc., Chem. Commun.* **1984**, 626. (m) Wakui, T.; Handa, T. *J. Chem. Soc., Chem. Commun.* **1984**, 994. (n) Chen, Y. W.; Wang, H. T.; Goodwin, J. G. *J. Catal.* **1984**, *85*, 499. (o) Tatsumi, T.; Odajima, H.; Tominaga, H. *J. Chem. Soc., Chem. Commun.* **1985**, 207. (p) Leith, I. R. *J. Catal.* **1985**, *91*, 283. (q) Oukaci, R.; Sayari, A.; Goodwin, J. G. *J. Catal.* **1987**, *106*, 318.

0020-1669/88/1327-3024$01.50/0

has been much less studied, in large part presumably because methane is normally the only product obtained over most supported ruthenium catalysts.[2] Relatively little is known concerning the effects of catalyst precursor, dispersion, and nature of the support on CO_2 hydrogenation, and although hydrogenation of CO_2 probably occurs via the intermediacy of sorbed CO,[2g,h,l,2m] details of the mechanism remain obscure.[4h] For both CO and CO_2 hydrogenation, the effects of varying the catalyst precursors, the reaction conditions, the metal dispersion, and the nature of the support have been investigated in depth.[3-5] There have also been extensive spectroscopic investigations of the nature of the species formed on sorption of ruthenium carbonyl clusters such as $Ru_3(CO)_{12}$ on oxide supports.[6]

We have earlier shown that catalysts based on $Ru_3(CO)_{12}$ are very effective for the hydrogenation of both CO and CO_2 at atmospheric pressure.[2j,k] We have now extended this work to a much wider investigation of CO and CO_2 hydrogenation by various ruthenium clusters at higher pressures, with particular attention to the possible effects of a novel method for encapsulating $Ru_3(CO)_{12}$ in the pores of a zeolite. We also describe experiments designed to throw light on the mechanism of the hydrogenation of CO_2. Aspects of this work have appeared previously.[7]

Experimental Section

Infrared (IR) spectra were run on a Bruker IFS 85 FTIR spectrometer. Catalyst testing was performed for the most part under essentially differential conditions in a Chemical Data Systems 803 Micro Pilot Plant stainless steel fixed-bed reactor with an on-line HP 5880A gas chromatograph equipped with both TC and FI detectors and *n*-octane Porasil-C, Porapak Q, and OV-101 columns.

All supports used (γ-alumina, Na–Y zeolite, and Linde 5A molecular sieve) were purchased from Strem Chemicals as $^1/_{16}$-in. pellets and were dried at 500 °C and 10^{-2} mm pressure for 24 h prior to catalyst loading. The compounds $Ru_3(CO)_{12}$[8] (I), $Na[HRu_3(CO)_{11}]$[9] (II), $[PPN][HRu_3(CO)_{11}]$[9] (III), $H_4Ru_4(CO)_{12}$[10] (IV), and $Ru_6(CO)_{18}Cu_2(toluene)_2$[11] (V) were prepared as in the literature. Impregnation onto γ-alumina was achieved by dissolving each cluster in pentane or methanol (for anionic clusters), filtering the solution into a flask containing the support under nitrogen, and allowing the mixture to stir for 2 h. The solvent was then removed under reduced pressure, and the supported catalyst was dried in vacuo for several hours at room temperature. Catalysts prepared in this way were generally pretreated in the reactor tube with flowing hydrogen (20 mL/m) at 200 °C for 20 h before use and contained 2–5% Ru by weight.

The cluster $Ru_3(CO)_{12}$ was introduced into the supercages of the Na–Y zeolite by vapor impregnation of the unstable monomer $Ru(CO)_5$, which was synthesized by published thermal and photochemical procedures.[12] In a typical experiment, 0.21 g of solid $Ru_3(CO)_{12}$ and 5 g dried Na–Y zeolite were treated with 200 atm of CO at 160 °C in a Superpressure Micro Series reactor. After 12 h the reactor was allowed to cool, and the zeolite pellets were transferred quickly to a nitrogen-filled flask as they turned from colorless to orange. Alternatively, treatment of the zeolite/$Ru_3(CO)_{12}$ mixture with 80 atm of CO in a Parr Stirring Minireactor gave the same results, although a longer time period (48 h) was required.

An alternative procedure involved the treatment of a suspension of 0.28 g of $Ru_3(CO)_{12}$ in 200 mL of *n*-decane with 80 atm of CO in a Parr Stirring Minireactor at 150 °C for 3 h. The resulting colorless or very pale yellow solution was then transferred under CO to a distillation apparatus, and $Ru(CO)_5$ (with some decane) was fractionally distilled at room temperature and 4 mmHg pressure into a flask containing dried zeolite cooled to −78 °C. On back-filling of the collection flask with nitrogen and warming to room temperature, the zeolite pellets changed from colorless to orange.

The $Ru_3(CO)_{12}$/zeolite catalyst precursors, which contained 2–5% Ru by weight, were subjected to two alternative pretreatment procedures. Procedure A involved rapid heating of the $Ru_3(CO)_{12}$/zeolite catalyst from room temperature to 200 °C in a reactor tube under flowing hydrogen (20 mL/min, 21 atm). The sample was then held at 200 °C under the hydrogen flow for 20 h. Procedure B involved treatment of the $Ru_3(CO)_{12}$/zeolite catalyst under vacuum (10^{-2} mmHg) or flowing hydrogen (20 mL/min, 21 atm) in the reactor tube, with temperature-programmed heating (1 °C/min) from room temperature to 350 °C. The catalyst sample was then held at 350 °C under hydrogen for 3–12 h.

Catalytic runs were typically performed with 1.4 g of catalyst at 21 atm and a gas hourly space velocity (GHSV) of 1000 h^{-1}. Ratios of H_2:CO and H_2:CO_2 were varied in the range 1:1 to 4:1, with temperatures in the range 150–320 °C. Steady-state product distributions and CO or CO_2 conversions were normally achieved within 24 h, and runs were typically of 4–5 days' duration.

Results and Discussion

Zeolite-Supported Catalysts. (1) Catalyst Preparation. Monomeric, colorless $Ru(CO)_5$ has been synthesized essentially quantitatively by the carbonylation of $Ru_3(CO)_{12}$ via both photochemical and thermal procedures[12] and has been characterized by its IR spectrum[8,12] (ν_{CO} 2037 (s), 2001 (vs) cm^{-1} in cyclohexane). Although the monomeric pentacarbonyl appears to be rapidly sorbed into Na–Y zeolite to give a colorless, $Ru(CO)_5$-containing zeolite catalyst precursor, the system rapidly loses CO when exposed to an atmosphere of nitrogen rather than CO, as is suggested by the observation of a rapid color change of the loaded zeolite from colorless to orange, the color of $Ru_3(CO)_{12}$. It has been reported, and we have confirmed, that the monomeric pentacarbonyl is unstable with respect to quantitative conversion to $Ru_3(CO)_{12}$ in hydrocarbon solution in the absence of added CO.[14] Interestingly, it has also been reported that Na–Y absorbs precisely three molecules of the slightly smaller $Fe(CO)_5$,[15] suggesting that the formation of $Ru_3(CO)_{12}$ occurs with ease in part because a zeolite supercage can hold three molecules of the pentacarbonyl precursor. Indeed, it is our experience that $Ru(CO)_5$ converts to the trimer more rapidly in the zeolite than in solution.[14]

More direct evidence that $Ru(CO)_5$ does indeed sorb into the Na–Y has been obtained from IR studies. Samples of the colorless pellets loaded with $Ru(CO)_5$ as described in the Experimental Section were handled in a CO-filled glovebag; under these conditions, the pellets became orange only over about a 15-min period.

---

(6) (a) Bowser, W. M.; Weinberg, W. H. *J. Am. Chem. Soc.* **1980**, *102*, 4720. (b) Kuznetsov, V. L.; Bell, A. T.; Yermakov, Y. I. *J. Catal.* **1980**, *65*, 374. (c) Zecchina, A.; Guglielminotti, E.; Bossi, A.; Camia, M. *J. Catal.* **1982**, *74*, 225. (d) Zecchina, A.; Guglielminotti, E.; Bossi, A.; Camia, M. *J. Catal.* **1982**, *74*, 240. (e) Zecchina, A.; Guglielminotti, E.; Bossi, A.; Camia, M. *J. Catal.* **1982**, *74*, 252. (f) Goodwin, J. G.; Naccache, C. *J. Mol. Catal.* **1982**, *14*, 259. (g) Theolier, A.; Choplin, A.; D'Ornelas, L.; Basset, J.-M.; Zanderighi, G.; Ugo, R.; Psaro, R.; Sourisseau, C. *Polyhedron* **1983**, *2*, 119. (h) Evans, J.; McNulty, G. S. *J. Chem. Soc., Dalton Trans.* **1984**, 1123. (i) Schay, Z.; Lázár, K.; Mink, J.; Guczi, L. *J. Catal.* **1984**, *87*, 179. (j) Asakura, K.; Yamada, M.; Iwasawa, Y.; Kuroda, H. *Chem. Lett.* **1985**, 511. (k) Zanderighi, G. M.; Dossi, C.; Ugo, R.; Psaro, R.; Theolier, A.; Choplin, A.; D'Ornelas, L.; Basset, J.-M. *J. Organomet. Chem.* **1985**, *296*, 127. (l) Dobos, S.; Böszörményi, I.; Silberer, V.; Guczi, L.; Mink, J. *Inorg. Chim. Acta* **1985**, *96*, L13. (m) Hunt, D. J.; Moyes, R. B.; Wells, P. B.; Jackson, S. D.; Whyman, R. *J. Chem. Soc., Faraday Trans. 1* **1986**, *82*, 189. (n) Sabbadini, M. G. C.; Gervasini, A.; Morazzoni, F.; Strumulo, D. *J. Chem. Soc., Faraday Trans. 1* **1986**, *83*, 2271. (o) Alexiev, V. D.; Binstead, N.; Evans, J.; Greaves, G. N.; Price, R. J. *J. Chem. Soc., Chem. Commun.* **1987**, 395.

(7) Hastings, W. R.; Thomas, M. J.; Cameron, C. J.; Baird, M. C. *Prepr.—Can. Symp. Catal., 10th* **1986**, 476.

(8) Eady, C. R.; Jackson, P. F.; Johnson, B. F. G.; Lewis, J.; Malatesta, M. C.; McPartlin, M.; Nelson, W. J. H. *J. Chem. Soc., Dalton Trans.* **1980**, 383.

(9) Johnson, B. F. G.; Lewis, J.; Raithby, P. R.; Süss, G. *J. Chem. Soc., Dalton Trans.* **1979**, 1356.

(10) Knox, S. A. R.; Koepke, J. W.; Andrews, M. A.; Kaesz, H. D. *J. Am. Chem. Soc.* **1975**, *97*, 3942.

(11) Bradley, J. S.; Pruett, R. L.; Hill, E.; Ansell, G. B.; Leonowicz, M. E.; Modrick, M. A. *Organometallics* **1982**, *1*, 748.

(12) (a) Huq, R.; Poë, A. J.; Chawla, S. *Inorg. Chim. Acta* **1980**, *38*, 121. (b) Rushman, P.; van Buuren, G. N.; Shiralian, M.; Pomeroy, R. K. *Organometallics* **1983**, *2*, 693.

(13) Johnson, B. F. G.; Lewis, J.; Nelson, W. J. H.; Nicholls, J. N.; Puga, J.; Raithby, P. R.; Rosales, M. J.; Schröder, M.; Vargas, M. D. *J. Chem. Soc., Dalton Trans.* **1983**, 2447.

(14) On the basis of qualitative, visual observations, the conversion is more rapid within the zeolite than in solution for approximately equal concentrations of $Ru(CO)_5$ (minutes rather than hours). This is probably because dissociated CO can escape more effectively from the zeolite than from solution. Preliminary kinetics studies show that the reaction is retarded very effectively by free CO.

(15) Bein, T.; Jacobs, P. A. *J. Chem. Soc., Faraday Trans. 1* **1983**, *79*, 1819.

Table I. Results of CO Hydrogenation Experiments over Catalysts α, β, and γ[a,b]

catalyst	% CO conversion[c] to hydrocarbons	% CO conversion[c] to CO_2	rel mol % C_1	rel mol % C_2	rel mol % C_{3+}	rel mol % C_{max}	olefin content[d] C_2	olefin content[d] C_3	olefin content[d] C_4
α	3.0	0.5	67	5	28	C_{20}	0.47	0.74	0.72
β	4.2	0.8	49	6	45	C_{16}	0.39	0.70	0.73
γ	4.0	2.0	66	8	28	C_{11}	0.52	0.68	0.52

[a] Catalysts α, β, and γ were prepared as described in the Experimental Section. [b] Catalytic conditions: P = 320 psig, T = 200 °C, GHSV = 1000 h^{-1}, H_2:CO = 1:1. [c] Total conversions 3.5–6%. [d] Olefin content = no. of moles of olefin of carbon no. *n*/total hydrocarbon of carbon no. *n*.

FTIR spectra of freshly prepared Nujol mull samples were run quickly and were found to contain broad absorptions at 2134 (w), 2079 (w, sh), 2062 (m), 2043 (s), 2021 (m), 2002 (w), and 1987 (w, sh) cm^{-1}. This rather complicated spectrum is very similar to that reported by Bein and Jacobs[15] for $Fe(CO)_5$ in Na–Y zeolite. $Ru(CO)_5$ and $Fe(CO)_5$ are both trigonal-bipyramidal molecules and exhibit very similar IR spectra in cyclohexane solution (ν_{CO} 2037 (s) and 2001 (vs) and ν_{CO} 2023 (s) and 2000 (vs) cm^{-1}, respectively). It has been proposed that the IR spectrum of $Fe(CO)_5$ is much more complicated in the zeolite than in solution because of weak interactions of the carbonyl oxygen lone pairs with Lewis acid sites within the zeolite;[15] similar interactions would be expected for the larger $Ru(CO)_5$. Frequency shifts and activation of otherwise IR-inactive vibrational modes ensue, apparently for the ruthenium analogue also.

The conversion of $Ru(CO)_5$ to $Ru_3(CO)_{12}$, as evidenced by the development of an orange coloration of the pellets, involved significant changes also in the Nujol mull IR spectra of the pellets. The spectral features attributed to sorbed $Ru(CO)_5$ disappeared, giving rise to a series of absorptions at 2167 (w), 2135 (w), 2123 (w), 2103 (m, sh), 2075 (s, br), 2040 (m, sh), 2002 (w, sh), and 1974 (w, sh) cm^{-1}, which correspond to those reported elsewhere[6b,c,f,h,l] for adsorbed $Ru_3(CO)_{12}$.

It seems clear from the above results that the relatively small $Ru(CO)_5$ (molecular diameter 6.3 Å) can diffuse readily into the pores (diameter 7.4 Å) and supercages (diameter 13 Å) of the zeolite.[16] In the absence of a partial pressure of CO, however, this monomer converts to the cluster $Ru_3(CO)_{12}$ (molecular diameter 9.2 Å), which, although small enough to fit inside the zeolite supercage, is presumably too large to pass through the zeolite pores.[5j] Relevant to this point are observations that similar experiments with 200 atm of nitrogen at room temperature and 100 °C did not lead to coloration of the pellets, while experiments under nitrogen at temperatures >100 °C resulted in decomposition of $Ru_3(CO)_{12}$ to give a black material (ruthenium metal?) and a brown cluster that extracted into chloroform (ν_{CO} 2072 (s, sh), 2068 (s), 2035 (m) cm^{-1}). The compound is probably $Ru_5C(CO)_{16}$[13] (ν_{CO} 2077 (m), 2057 (s), 2028 (m) cm^{-1} (hexane)). The failure of $Ru_3(CO)_{12}$ to sublime into Na–Y zeolite at 100 °C under nitrogen rather than CO pressure strongly implies that loading occurs only via $Ru(CO)_5$, and we are sceptical of a literature claim that $Ru_3(CO)_{12}$ has been successfully sorbed into Na–Y zeolite.[5e] We note that others have also found that $Ru_3(CO)_{12}$ does not diffuse into Na–Y zeolite.[5j]

Interestingly, attempts to sublime $Ru(CO)_5$ into the pores of Linde 5A molecular sieve (kinetic pore diameter 4.2 Å[16]) apparently failed, as tetrahydrofuran readily leached $Ru_3(CO)_{12}$ from the molecular sieve after impregnation with $Ru(CO)_5$. Furthermore, a Nujol mull spectrum of the residual $Ru_3(CO)_{12}$ on Linde 5A was very similar to the IR spectrum of a Nujol mull of unsupported $Ru_3(CO)_{12}$ but very different from that of $Ru_3(CO)_{12}$ sorbed in Na–Y zeolite (which could not be extracted with tetrahydrofuran). The Linde 5A material also exhibited very different catalytic properties (see below).

Temperature-programmed decomposition of Na–Y-sorbed $Ru_3(CO)_{12}$ was studied by IR spectroscopy. Heating to 150 °C resulted in disappearance of the carbonyl bands attributed to $Ru_3(CO)_{12}$ and appearance of broad features at about 2050, 1969, and 1950 cm^{-1}, assignments of which are subject to controversy.[6]

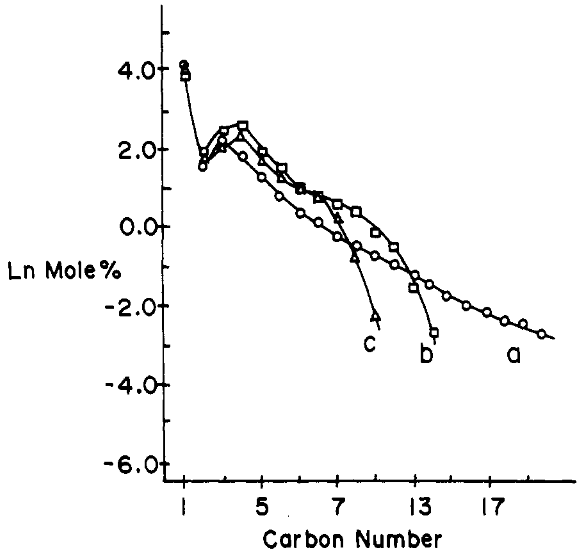

Figure 1. Anderson–Schulz–Flory plots for catalysts α (a), β (b), and γ (c) (conditions as in Table I).

The latter absorptions were still very apparent at 280 °C but had disappeared by 350 °C, suggesting that catalysts prepared by our pretreatment procedure A (rapid heating to 200 °C under flowing hydrogen) were probably not completely decarbonylated. In contrast, catalysts prepared by pretreatment procedure B (slow heating to 350 °C under flowing hydrogen) would be completely decarbonylated. The possible implications of these inferences will be discussed below.

Catalysts for CO and CO_2 hydrogenation were synthesized via essentially two preparative and two pretreatment procedures, as described in the Experimental Section. Catalysts hereafter designated α and β were prepared by sorbing $Ru(CO)_5$ into Na–Y zeolite at high temperature (160 °C) and pressure (200 atm), and catalyst γ was prepared by sorbing distilled $Ru(CO)_5$ into Na–Y zeolite at room temperature, i.e. under significantly milder conditions. Subsequent pretreatment of α involved the above-described procedure A, i.e. rapid heating of the sample to 200 °C. In contrast, catalysts β and γ underwent procedure B, which involved temperature-programmed heating (1 °C/min) to 350 °C, a much milder treatment in the initial stages. Thus, the three classes of catalysts, α, β and γ, were prepared under conditions of decreasing severity, in that order.

(2) Carbon Monoxide Hydrogenation. Studies of the hydrogenation of CO, catalyzed by the three classes of catalysts, were carried out under a variety of conditions, as outlined in the Experimental Section. Typical results are presented in Table I, and representative product distributions are shown in Figure 1 as Anderson–Schulz–Flory (ASF) plots. Methane was a major product in all cases, although significant amounts of *n*-alkanes, isoalkanes, and olefinic (up to 75% of the total for C_3) hydrocarbons were also obtained. Increasing the temperature and the H_2:CO ratio resulted in increased methane production, although altering the total pressure by a factor of 2 had little effect on product distributions.

It was found that catalyst α exhibited a CO conversion and nonselective product distribution typical of those reported elsewhere both for $Ru_3(CO)_{12}$-on-Na–Y catalysts[5j,o] and for poorly dispersed catalysts derived from ruthenium compounds on non-

---

(16) Breck, D. W. *Zeolite Molecular Sieves*; Wiley: New York, 1974.

zeolitic supports at medium pressure.[2c,3b,g] Indeed, the ASF plot for catalyst α (Figure 1a) is typical of those of many Fischer–Tropsch catalysts based on transition metals, including ruthenium.[1] A CO conversion of about 6% was maintained for 4 days with this catalyst, and olefins constituted 40–60% of the total hydrocarbons, a proportion typical of many ruthenium-based Fischer–Tropsch catalysts.[3b,e,h,4c,g,5j,k,n] Furthermore, the *n*-butane:isobutane ratio was 4.0; isoalkanes are atypical products of ruthenium-based CO hydrogenation catalysts but have been observed for ion-exchanged Ru/Na–Y systems.[5k,n]

Interestingly, catalysts β and γ, which were prepared under increasingly milder conditions in that order, produced atypical product distributions (Figure 1b,c, respectively). This is especially true of catalyst γ, which exhibited a dramatic truncation of the products at C_9, corresponding approximately to the dimensions of the Na–Y supercage. The length of time over which this selective product distribution was observed (up to 4 days) precludes the possibility that a transient phenomenon such as retention of higher hydrocarbons by zeolite was responsible. In addition, the observation of normal ASF product distributions, with similar conversions, early in runs involving catalyst α is evidence that the shape selectivity described above is a true cage effect and not a transient phenomenon.

For catalyst β, olefin proportions and CO conversions were much as for catalyst α, although the *n*-butane:isobutane ratio was somewhat lower (2.2). For catalyst γ, the CO conversion was similar, but the *n*-butane:isobutane ratio (0.46) and the olefin proportions were somewhat lower.

The ASF profile for catalyst γ is very similar to that observed for a Ru/Na–Y system prepared by ion exchange with $[Ru(NH_3)_6]Cl_3$,[5a,b] and it is interesting to note that a Fischer–Tropsch catalyst containing ruthenium supported on silica having a pore diameter less than 20 Å and very narrow pore size distribution also gives rise to non-ASF behavior, with a truncation in the C_9–C_{11} region.[5m] The precise nature of the apparent cage effect, whether it arises from the pore size restrictions on chain growth or from a particular ruthenium particle size distribution induced by the support, cannot be defined with confidence, as it is becoming increasingly apparent that Fischer–Tropsch product distributions are sensitive to many subtle factors having to do with the mode of catalyst preparation.[17]

However, similar distributions have also been observed for catalysts based on $Fe_3(CO)_{12}$[5e,19] and $Co_2(CO)_8$[19] in Na–Y, and the fact that different metal catalyst systems give rise to a common cutoff point corresponding to the dimensions of the Na–Y supercage suggests the operation of a cage effect. In addition, the product distribution exhibited by catalyst γ is novel for $Ru_3(CO)_{12}$/Na–Y systems; no shape selectivity has been observed for $Ru_3(CO)_{12}$/Na–Y catalysts prepared under conditions[5e,j,o] that our results suggest cannot involve vapor impregnation of the cluster within the zeolite supercages. The novel loading procedure described here, in which the smaller, more volatile $Ru(CO)_5$ is employed, is the first to ensure that $Ru_3(CO)_{12}$ is formed within and is immobilized by the zeolite supercage.

In contrast, catalysts α and β were formed under conditions in which $Ru(CO)_5$ could diffuse into the zeolite pores but at a sufficiently high temperature (200 °C) that thermal degradation of either the $Ru(CO)_5$ or the $Ru_3(CO)_{12}$ to which it was being transformed could also lead to immobilization of some of the ruthenium on the outside surfaces of the support.[6] In addition, catalyst α underwent a pretreatment procedure involving very rapid heating of only partially decarbonylated material, and it would appear that extensive migration of metal out of the supercages had occurred. In any case, the catalytic behavior of the system was clearly not dominated by intracage catalyst sites. Catalyst β, which was prepared under the forcing conditions of catalyst α but pretreated under the mild conditions of catalyst γ, exhibited bimodel behavior characteristics of the presence of two distinctly different types of sites[18] and/or of a catalyst with both surface and supercage active sites.[19]

Table II. Results of CO_2 Hydrogenation over Catalyst α and a Catalyst Prepared by Supporting $Ru_3(CO)_{12}$ on Linde 5A Molecular Sieve[a]

catalyst	% conversion (±5%)	prod. distribn, mol % C_1	C_2	C_{3+}	C_{max}
α	100	99.8	0.2		C_2
Ru/Linde 5A	92	99.5	0.5		C_2

[a] P = 200–320 psig, GHSV = 1000 h^{-1}, T = 320 °C, H_2:CO_2 = 4:1.

Table III. Results of CO_2 Hydrogenation over Catalysts α and γ[a]

	% conversion		rel mol %			
catalyst	to hydrocarbons	to CO	C_1	C_2	C_{3+}	C_{max}
α[b]	25	0	97	1.8	1.2	C_{16}
γ[c]	4.2	2.8	90.2	5.0	4.8	C_{11}

[a] P = 320 psig, T = 200 °C, GHSV = 1000 h^{-1}, H_2:CO_2 = 1:1. [b] Total conversion 25%. [c] Total conversion 7%.

Interestingly, a catalyst prepared by sorbing $Ru(CO)_5$ onto the small pore Linde 5A molecular sieve exhibited a nonselective hydrocarbon product distribution very similar to that observed for catalyst α. In the molecular sieve system, the ruthenium clearly existed only on the external surface of the support. In addition, catalyst γ appeared to begin to lose some of its selectivity after 50 h on stream, as heavier hydrocarbons began to appear. It has been reported that ruthenium volatilization via carbonyl formation can occur in systems similar to those studied here,[20] providing a mechanism for migration of the metal to the zeolite surface. Thus the product selectivities exhibited to varying degrees by catalysts β and γ seem best rationalized on the basis of cage-encapsulated ruthenium particles. Consistent with this conclusion, it was found that a catalyst loaded into Na–Y zeolite as per catalyst α, but then treated with methyl iodide, exhibited reduced activity and a product selectivity very similar to that of catalyst γ. This behavior, not noted previously by others who have done similar experiments,[5o] may be attributed to selective poisoning of the ruthenium on the surface, leaving only catalytic sites within the pores of the zeolites. Unfortunately, we did not observe the C_2 enhancement reported elsewhere.[5o]

All three catalyst systems, α, β, and γ, produced significant quantities of isobutane, a property heretofore associated only with ruthenium catalysts formed by ion-exchange impregnation into zeolite pores.[5k,n] The interpretation to be given these results is not clear.

(3) Carbon Dioxide Hydrogenation. CO_2 hydrogenation experiments were carried out by using the same catalyst systems (α, β, γ) described above, but under two distinct sets of reaction conditions. Those discussed first have involved high temperatures and H_2:CO_2 ratios, conditions under which methanation is the dominant reaction, in order to compare the catalyst activities and selectivities with those of previously studied, very active CO_2 methanation catalysts.[2j,k,m] Experiments were also carried out under conditions designed to favor the formation of higher hydrocarbons, which are not normally obtained from CO_2 hydrogenation. Interesting comparisons with the properties of catalysts α, β and γ as CO hydrogenation catalysts became possible, leading to information pertinent to the mechanism of CO_2 hydrogenation.

As indicated in Table II, catalyst α and the $Ru_3(CO)_{12}$/Linde 5A catalyst were both superb CO_2 methanation catalysts at 320 °C, producing methane but very little CO and C_2–C_4 hydrocarbons; both catalysts exhibited CO_2 conversions nearing 100%,

---

(17) For discussions, see ref 5p, 5q, and 18.

(18) Jacobs, P. A. In *Catalysis by Zeolites*; Imelik, B., Naccache, C., Ben Taarit, Y., Vedrine, J. C., Coudurier, G., Praliaud, H., Eds.; Elsevier: Amsterdam, 1980; p 293.

(19) Ballivet-Tkatchenko, D.; Chau, N. D.; Mozzanega, H.; Roux, M. C.; Tkatchenko, I. In *Catalytic Activation of Carbon Monoxide*; Ford, P. C., Ed.; ACS Symposium Series 152; American Chemical Society: Washington, DC, 1982; p 187.

(20) Goodwin, J. G.; Goa, D. O.; Erdal, S.; Rogan, F. H. *Appl. Catal.* **1986**, *24*, 199.

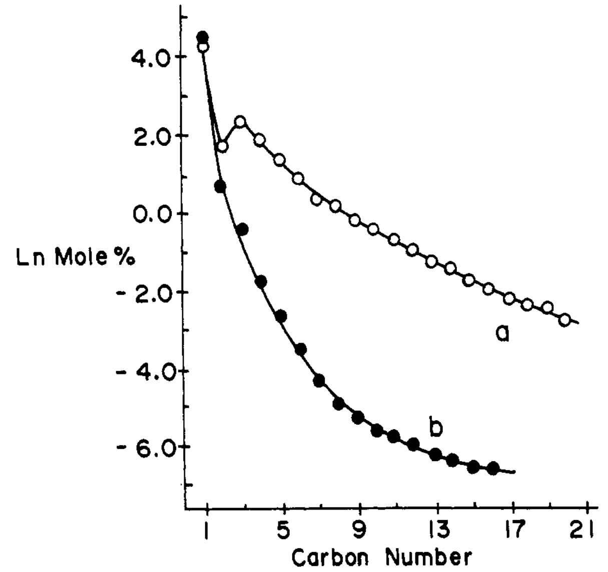

Figure 2. Anderson–Schulz–Flory plots for CO hydrogenation (a) and CO_2 hydrogenation (b) over catalyst α (conditions as in Tables I and III).

essentially independent of the total pressure (1, 8, 22 atm). The conversions were temperature-dependent for both the Na–Y supported and Linde 5A supported materials, and an Arrhenius plot of the latter system gave an activation energy of 30 ± 2 kJ/mol in the temperature range 150–240 °C. This value is probably less certain than suggested because no precautions were taken to minimize heat-transfer effects, but linearity in the Arrhenius plot was achieved in the temperature ranged noted. The value determined is at the lower end of the range of activation energy data that have been reported for supported ruthenium CO_2 methanation catalysts ($\approx$41–103 kJ/mol);[2g,h,l,4h] there appears to be as yet no rationale for the widely varying values.

Attempts to minimize methane formation and to enhance the formation of higher hydrocarbons were made under typical Fischer–Tropsch conditions (200 °C, 20 atm, H_2:CO_2 = 1:1). Our initial experiments involved the use of catalyst α, which was very nonselective for CO hydrogenation. As shown in Table III, small but significant amounts of up to C_{16} hydrocarbons formed, a result apparently without precedent in the literature for CO_2 hydrogenation. The product distribution obtained is illustrated as an ASF plot in Figure 2, where it is compared with the profile obtained with the same catalyst for CO hydrogenation. The amount of C_2 and higher hydrocarbons is very much lower for CO_2 hydrogenation, but the more significant observation is that the two profiles are strikingly different. Absence of the C_2 depletion observed for CO hydrogenation and characteristic of many Fischer–Tropsch catalysts is particularly noteworthy; in addition, no olefins or isoalkanes were observed in the case of CO_2 hydrogenation. These experiments were entirely reproducible, both in separate experiments with the two carbon oxides and in experiments in which the H_2–CO and H_2–CO_2 feed gases were repeatedly alternated with the same catalyst sample on stream.

In an attempt to demonstrate for the first time shape selectivity during CO_2 hydogenation, a run was made by using catalyst γ; the results are shown in Table III but are inconclusive. A cutoff point may exist at C_{11}, but the small amounts of hydrocarbons formed are near the limits of GC detection.

(4) Mechanistic Considerations. Differences in activities and product distributions have been noted in the hydrogenation of CO and CO_2 over identical catalysts, suggesting at first sight that the two reactions proceed via different mechanisms. However, our results can nevertheless be rationalized within the prevailing view that CO_2 hydrogenation proceeds via initial transformation of adsorbed CO_2 to adsorbed CO and oxygen, followed by dissociation of the CO to active carbidic carbon, which is in turn hydrogenated.[2h,l,4h] Thus, the hydrogenations of CO and CO_2 would both involve the same active carbon intermediates(s).

Table IV. CO and CO_2 Hydrogenation by γ-Al_2O_3-Supported Ruthenium Carbonyl Clusters[a]

	catalyst						
	I		II		III	IV	V
reacting gas	CO_2	CO	CO_2	CO	CO_2	CO_2	CO_2
conversion, %	9	4	9	4	2	9	23
rel mol %							
C_1	97	65	96	65	96	98	97
C_2	3	7	3	8	4	2	3
C_{3+}	0.3	28	1	27	0.2	0.4	0.5
C_{max}	C_{15}	C_{22}	C_{10}	C_{21}	C_3	C_{16}	C_{15}
tot. % olefins	0	20	0	20	0	0	0

[a] Activated at 350 °C under H_2 flow unless stated otherwise; 1–2% Ru; H_2:CO_2 or H_2:CO 1:1; temperature 220 °C and GHSV = 1700 h^{-1}.

It has been determined that the concentration of adsorbed CO and active carbide species on a supported ruthenium catalyst surface is significantly lower during CO_2 than during CO hydrogenation, resulting in much higher surface hydrogen concentrations during hydrogenation of CO_2.[2h] If the rate-determining steps of both CO and CO_2 hydrogenation processes involve hydrogenation of the active carbon,[2h] the localized, relatively hydrogen-rich environment at the active sites during CO_2 hydrogenation would be expected to increase the proportion of methane formed relative to the amount formed during CO hydrogenation. As we have demonstrated here for the first time, extensive hydrocarbon chain growth can occur during CO_2 hydrogenation, but this result in fact provides further evidence for the validity of the proposed mechanism. No olefins are observed during CO_2 hydrogenation, consistent with there being a relatively high hydrogen concentration; if olefins are formed, they are rapidly hydrogenated, in contrast to behavior during CO hydrogenation. In addition, there is no deficiency of ethane in the ASF plot illustrated for CO_2 hydrogenation in Figure 2; if ethylene is formed, it is hydrogenated rather than incorporated into growing hydrocarbon chains as is believed to occur during CO hydrogenation.[1a] The formation of branched hydrocarbons during CO but not during CO_2 hydrogenation may be rationalized similarly; secondary reactions involving incorporation of olefins into growing chains, to form branched isomers,[1a] will be prevented if olefin hydrogenation is rapid.

γ-Alumina-Supported Catalysts. The rationale behind the use of the various ruthenium carbonyl clusters followed our earlier low-pressure studies[2j,k] involving $Ru_3(CO)_{12}$ (I) and was based in part on reports of promoter effects on CO hydrogenation. For instance, $Na[HRu_3(CO)_{11}]$ (II) was studied because sodium is known to be a catalytic promoter of chain growth and olefin formation;[4f] $[PPN][HRu_3(CO)_{11}]$ (III), for purposes of comparison. $H_4Ru_4(CO)_{12}$ (IV) has been shown to exhibit unusual product distributions in CO hydrogenation experiments.[4d] Thus it seemed worthwhile to investigate the possibility of these interesting properties being carried over into CO_2 catalytic hydrogenation. In addition, copper is involved in the catalytic conversion of CO_2 to methanol,[21] and it seemed possible that the bimetallic copper–ruthenium cluster, $Ru_6(CO)_{18}Cu_2(toluene)_2$ (V), might form oxygenates from CO_2 hydrogenation.

The results of several comparative experiments are shown in Table IV. As can be seen, the results were generally disappointing, although again rather long hydrocarbon chains were obtained during CO_2 hydrogenation over most of the clusters.

Acknowledgment. This research was supported by the U.S. Office of Naval Research. We are also indebted to Johnson-Matthey Ltd. and the International Nickel Co. of Canada for loans of ruthenium chloride and to M. Woods, S. Binks, and L. Christie for assistance in catalyst testing.

---

(21) Denise, B.; Sneeden, R. P. A. *CHEMTECH* **1982**, 108.